THE JOURNAL OF BIOLOGICAL CHEMISTRY
Vol. 277, No. 6, Issue of February 8, pp. 4079–4087, 2002

Printed in U.S.A.

A Novel Leucine Zipper Targets AKAP15 and Cyclic AMP-dependent Protein Kinase to the C Terminus of the Skeletal Muscle Ca^{2+} Channel and Modulates Its Function*

Received for publication, October 10, 2001, and in revised form, November 23, 2001
Published, JBC Papers in Press, November 30, 2001, DOI 10.1074/jbc.M109814200

Joanne T. Hulme‡, Misol Ahn‡, Stephen D. Hauschka§, Todd Scheuer‡, and William A. Catterall‡¶

From the Departments of ‡Pharmacology and §Biochemistry, University of Washington, Seattle, Washington 98195-7280

In skeletal muscle, voltage-dependent potentiation of L-type Ca^{2+} channel ($Ca_V1.1$) activity requires phosphorylation by cyclic AMP-dependent protein kinase (PKA) anchored via an A kinase-anchoring protein (AKAP15). However, the mechanism by which AKAP15 targets PKA to L-type Ca^{2+} channels has not been elucidated. Here we report that AKAP15 directly interacts with the C-terminal domain of the α_1 subunit of $Ca_V1.1$ via a leucine zipper (LZ) motif. Disruption of the LZ interaction effectively inhibits voltage-dependent potentiation of L-type Ca^{2+} channels in skeletal muscle cells. Our results reveal a novel mechanism whereby anchoring of PKA to Ca^{2+} channels via LZ interactions ensures rapid and efficient phosphorylation of Ca^{2+} channels in response to local signals such as cAMP and depolarization.

In skeletal muscle, voltage-gated Ca^{2+} channels localized in the transverse tubule membrane play a pivotal role in excitation-contraction coupling (1). Following membrane depolarization during an action potential, these Ca^{2+} channels function as voltage sensors to initiate excitation-contraction coupling and as a slowly activating Ca^{2+} entry pathway that regulates contractile force (1–3). Trains of high frequency depolarizing stimuli that mimic action potentials or single long depolarizing pulses greatly increase the activity of these Ca^{2+} channels (4, 5). This "potentiation" of Ca^{2+} channel activity is strongly voltage-dependent and, in skeletal muscle, requires phosphorylation by PKA[1] (4). This novel regulatory mechanism most likely contributes to the overall regulation of contractile force in response to motor nerve stimulation (6, 7).

The importance of PKA anchoring through the association with AKAPs has recently been established in the regulation of L-type Ca^{2+} channels. AKAPs belong to a family of functionally related proteins, which contain a targeting domain that directs the AKAP to a specific subcellular compartment or substrate and a kinase-anchoring domain containing an amphipathic α-helix that binds the regulatory (R) subunit dimer of PKA (8–13). Dialysis of "kinase-anchoring inhibitor peptides" into cells, which competitively inhibit PKA-AKAP interactions, effectively reduces voltage-dependent potentiation of Ca^{2+} channel activity in skeletal muscle cells (12, 14, 15) and cloned skeletal Ca^{2+} channels expressed in human embryonic kidney cells (15). Thus, anchoring of PKA to L-type Ca^{2+} channels via an AKAP favors the rapid phosphorylation and modulation of these channels.

Recent biochemical studies of skeletal muscle Ca^{2+} channels have identified a novel low molecular weight AKAP, AKAP15 (12) (also known as AKAP18 (13)), that co-purifies, co-immunoprecipitates, and co-localizes with the skeletal muscle Ca^{2+} channel complex (12, 16, 17). The primary structure reveals an 81-residue protein containing an amphipathic helix that binds the regulatory subunit dimer of PKA and N-terminal palmitoyl and myristoyl moieties that target AKAP15 to the plasma membrane (12, 13).

Whereas AKAP15 has been implicated as the anchoring protein that targets PKA to the Ca^{2+} channel complex in skeletal muscle, the mechanism by which AKAP15 associates with L-type Ca^{2+} channels has not been elucidated. In the present study, we report that AKAP15 directly interacts with the C-terminal domain of the α_1 subunit of $Ca_V1.1$ and anchors PKA via a leucine zipper (LZ) interaction. Furthermore, we show that disruption of the LZ interaction between AKAP15 and the C-terminal domain of $Ca_V1.1$ effectively inhibits voltage-dependent potentiation of L-type Ca^{2+} channel activity in skeletal muscle cells. Our results reveal a novel mechanism whereby anchoring of PKA to L-type Ca^{2+} channels via an LZ interaction ensures rapid and efficient phosphorylation of Ca^{2+} channels in response to local signals such as cAMP and depolarization.

EXPERIMENTAL PROCEDURES

Antibodies, Peptides, and DNA Constructs—The polyclonal antibody anti-AP1 (AVQQYLEETQNK) and RII-biotin protein were prepared as described previously (16). Monoclonal anti-Myc antibody was purchased from Invitrogen (Carlsbad, CA). $AKAP15_{LZ}$(38–54) (acetyl-ENAVLKAVQQYLEETQN-amide) and $AKAP15_{LZM}$(38–54) peptides (acetyl-ENAVAKAVQQYAEETQN-amide) were synthesized and purified by Genemed Synthesis Inc. (San Francisco, CA). PKI(5–24)-amide was obtained from Peninsula Laboratories (San Carlos, CA), and AP2 peptide was synthesized and purified as described previously (12).

Molecular Biology—Sequences corresponding to the N terminus, NH_2(aa 1–71); the intracellular loops between domains I and II (LI–II, aa 355–452); II and III (LII-III, aa 662–799); III and IV (LIII-IV, aa 1066–1138); the C terminus (COOH, aa 1382–1873); and C-terminal fragments (CT1, CT2, CT3, CT4, CT5, CT6, CT7, and CT8) of the α_1 subunit of the rabbit skeletal muscle L-type Ca^{2+} channel were amplified by PCR with specific primers and cloned in frame into the Gal4

* This work was supported by an American Heart Association postdoctoral fellowship (to J. T. H.), by research grants from the Muscular Dystrophy Association, and by National Institute of Health Grants P01 HL 44948 (to W. A. C.) and R01 AR18860 (to S. D. H.). The costs of publication of this article were defrayed in part by the payment of page charges. This article must therefore be hereby marked "*advertisement*" in accordance with 18 U.S.C. Section 1734 solely to indicate this fact.

¶ To whom correspondence should be addressed: Dept. of Pharmacology, Box 357280, University of Washington, Seattle, WA 98195-7280. Tel.: 206-543-1925; Fax: 206-543-3882, E-mail: wcatt@u.washington.edu.

[1] The abbreviations used are: PKA, cAMP-dependent protein kinase A; ABD, AKAP15 binding domain in $Ca_V1.1$; AKAP, A-kinase anchoring protein; $Ca_V1.1$, skeletal muscle L-type Ca^{2+} channel α_1 subunit; GST, glutathione *S*-transferase; LZ, leucine zipper; NAc, N-terminal acylation sequence of AKAP15; R, regulatory subunit of PKA; aa, amino acid; 3-AT, 3-amino-1,2,4-triazole.

DNA binding domain vector, pAS2-1 (CLONTECH, Palo Alto, CA). Wild type (*wt*) and deletion constructs of AKAP15 were generated in the same manner and cloned in frame into the Gal4 activation domain vector, pACT2 (CLONTECH). N-terminal acylated (NAc) CT fragments of $Ca_V1.1$ were constructed by incorporating the myristoylation and palmitoylation sequence (MGALCC) of AKAP15 onto the N terminus of the CT fragments by PCR and cloned in frame into pcDNA3mycHisA (Invitrogen). For production of His fusion proteins, the CT fragments of $Ca_V1.1$ were sub-cloned into pET29a (Novagen, Madison, WI). Glutathione *S*-transferase (GST) fusion proteins of AKAP15 were made by sub-cloning AKAP15 into pGEX-3X (Amersham Biosciences). $Ca_V1.1$ ABD_{LZm}(V1793A/L1800A) and $AKAP15_{LZm}$(L42A/L49A) were constructed using PCR overlap extension and cloned into pcDNA3-mycHisA, pAS2-1, and pACT2, respectively. The orientation and reading frame of all constructs were confirmed by DNA sequencing.

Yeast Two-hybrid Assay—cDNA encoding different regions of the Ca^{2+} channel and AKAP15 were co-transformed into the Y190 yeast strain, containing two Gal4-inducible reporter genes, *HIS3* and *lacZ*, using the TRAFCO LiAc method. Co-transformants were first plated onto synthetic dropout medium lacking tryptophan and leucine (trp^-leu^-) to select for colonies containing both hybrid plasmids and then transferred onto medium that also lacked histidine ($trp^-leu^-his^-$) to select for protein-protein interactions. Media were supplemented with 30 mM 3-amino-1,2,4-triazole (3-AT) to suppress background growth of the Y190 yeast strain. Only those transformants that grew on $trp^-leu^-his^-$ media at 30 °C were assayed for β-galactosidase activity using the colony filter lift assay (18). Data shown are representative of at least four separate experiments.

Protein Expression and in Vitro Binding Assay—Fusion proteins were expressed in the *Escherichia coli* expression host BL21(DE3) (Novagen). His fusion proteins of $Ca_V1.1$ (CT3, CT4, and CT6) were expressed as soluble proteins and were purified on a nickel-nitrilotriacetic acid-agarose column (Qiagen, Valencia, CA). GST-AKAP15 was first purified on a GST column and then cleaved from GST using factor Xa (Amersham Biosciences). All fusion proteins were quantified by bicinchoninic assay. His-CT fusion proteins bound to nickel-nitrilotriacetic acid beads were incubated with 5 μg of cleaved AKAP15 for 3 h at 4 °C. Protein complexes bound to the beads were washed extensively in wash buffer (20 mM Tris-HCl, pH 7.4, 150 mM NaCl, 0.05% Triton X-100), and proteins were separated by SDS-PAGE and transferred onto nitrocellulose. Bound proteins were detected with anti-AP1 antibody (1/1000 (12)). Immunoblots containing 10% of the His fusion proteins used in the binding assay were probed with anti-His antibody (Invitrogen; 1/1000). Each *in vitro* binding assay was repeated at least three times.

Co-immunoprecipitation Experiments—TsA-201 cells were cultured in Dulbecco's modified Eagle's medium/Ham's F-12 supplemented with 10% fetal bovine serum, 100 units/ml penicillin and streptomycin plated on 15-cm dishes. Cells were transfected with 50 μg of an equimolar ratio of expression plasmid cDNA using the calcium phosphate method. 48 h post-transfection, cells were washed in phosphate-buffered saline, solubilized in ice-cold bRIA (50 mM Tris-HCl, pH 7.4, 150 mM NaCl, 1 mg ml^{-1} bovine serum albumin, 50 mM NaF, 5 mM EGTA, 5 mM EDTA, 1% Triton X-100, plus protease inhibitors), and rotated at 4 °C for 30 min. Unsolubilized material was removed by centrifugation, and lysates were pre-cleared with protein AG-Sepharose. Pre-cleared lysates were incubated with 2 μg of anti-Myc antibody (Invitrogen) or 2 μg of control non-immune IgG for 3 h at 4 °C, followed by the addition of protein AG-Sepharose (50 μl) for an additional 2 h. Immune complexes bound to the Sepharose beads were washed extensively, and proteins were separated by SDS-PAGE, transferred to nitrocellulose, and analyzed by immunoblotting. Myc-tagged NAc-CT fragments were detected using monoclonal anti-Myc antibody (Invitrogen). For AKAP15 detection, immunoblots were probed using the anti-AP1 antibody or the RII-biotin overlay assay (16). Each immunoprecipitation experiment was repeated at least three times.

Skeletal Myotube Cell Culture and Electrophysiology—The permanent clonally derived line of BALB/c mouse skeletal muscle cells, MM14, subline DZ1A, was grown exponentially in a medium consisting of 85% Ham's F-10C nutrients (Ca^{2+} adjusted to 1.26 mM and 60 mg/ml gentamicin), 15% pre-selected horse serum, and 3 ng/ml human recombinant basic fibroblast growth factor. Cultures were passaged using 0.05% trypsin plus EDTA (Invitrogen), resuspended in differentiation media (85% Ham's F-10C, 15% HS), and inoculated at final concentrations of 20,000 and 30,000 cells per 35-mm gelatin-coated culture dish (19). This protocol was designed to provide relatively sparse cell densities in which greater than 90% of the cells were differentiated within 24 h (determined by myosin heavy chain immunocytochemistry), but in which cell fusion was minimized. Recordings were made from elongated myotubes containing 2–4 myonuclei 48–72 h post-differentiation.

Barium currents through skeletal muscle Ca^{2+} channels were recorded from MM14 myotubes using the whole-cell configuration of the patch clamp technique. Patch pipettes (2.5–3.5 megohms) were pulled from micropipette glass (VWR Scientific, West Chester, PA) and fire-polished prior to use. Junction potentials were corrected after placing the tip of the electrode in the bath solution and before gigaohm seal formation, which was achieved via gentle suction. After establishing the whole-cell configuration, capacitative transients elicited by symmetrical 20-mV clamp steps from −80 mV were recorded to calculate cell capacitance and access resistance. Capacitative currents were measured and electronically compensated (>90%), and the remaining linear components were subtracted using a P/4 leak subtraction protocol. The average membrane capacitance for all experiments was 62.3 ± 2.3 picofarads (n = 41). Currents were recorded with an Axopatch 200B amplifier (Axon Instruments Inc., Union City, CA) and sampled at 5 kHz after anti-alias filtering at 2 kHz. Data acquisition and command potentials were controlled by pClamp software (version 8.0, Axon Instruments), and data were stored for later off-line analysis. The extracellular bath solution contained (in mM) 150 Tris, 1 $MgCl_2$, and 10 $BaCl_2$. The intracellular recording solution consisted of (in mM) 130 *N*-methyl-D-glucamine, 60 Hepes, 2 MgATP, and 1 $MgCl_2$. The pH of both solutions was adjusted to 7.3 with methanesulfonic acid (300–310 mosM l^{-1}). All experiments were performed at room temperature (21–23 °C). All data are expressed as the mean ± S.E. of n cells. Statistical significance was tested using Student's t test. Values of $p < 0.01$ were considered significant.

RESULTS

AKAP15 Directly Interacts with the C-terminal Domain of $Ca_V1.1$—Previous work has shown that AKAP15 co-immunoprecipitates and co-localizes with the skeletal muscle L-type Ca^{2+} channel in transverse tubule membranes (12, 16). However, the mechanism by which AKAP15 associates with the Ca^{2+} channel complex has not been elucidated. To examine the possibility that AKAP15 directly interacts with the skeletal muscle L-type Ca^{2+} channel ($Ca_V1.1$), the yeast two-hybrid system was used. cDNA encoding the intracellular loops of the α_1 subunit of $Ca_V1.1$ (Fig. 1*A*) and AKAP15 were co-transformed into the Y190 yeast strain using standard techniques. Positive interactions were assayed by growth on selective medium dependent on activation of the nutritional selection marker gene *HIS3* and by staining dependent on activation of the second reporter gene, *lacZ*, using the β-galactosidase assay. Fig. 1*B* shows that AKAP15 interacted with the C-terminal domain of the α_1 subunit of $Ca_V1.1$. This interaction was specific for the two proteins since neither AKAP15 nor the C-terminal domain of $Ca_V1.1$ activated reporter gene expression when co-transformed with empty vector alone (Fig. 1*B*, +pACT2). To identify the minimal region within the C terminus that interacted with AKAP15, a series of deletions spanning the C-terminal domain of $Ca_V1.1$ were generated (Fig. 1*C*), and their ability to interact with AKAP15 was assessed using the yeast two-hybrid assay. Deletion analysis revealed that a 68-amino acid AKAP15 binding domain (CT7; amino acids 1774–1841) in the distal half of the C terminus was sufficient to interact with AKAP15 (Fig. 1*D*).

To confirm this interaction *in vitro*, bacterially expressed His fusion proteins encompassing different regions of the C-terminal domain of $Ca_V1.1$ were immobilized on nickel-nitrilotriacetic acid-agarose and incubated with cleaved AKAP15. Following extensive washing, bound proteins were eluted and analyzed by SDS-PAGE and immunoblotting. As shown in Fig. 2, AKAP15 bound specifically to CT4 and CT6, which contain residues 1774–1841, but not CT3, which lacks this sequence. Hexahistidine-tagged fusion proteins of the intracellular loops I–II and II–III also failed to bind AKAP15 in this assay and served as negative controls (data not shown). These *in vitro* binding data suggest that AKAP15 directly interacts with the

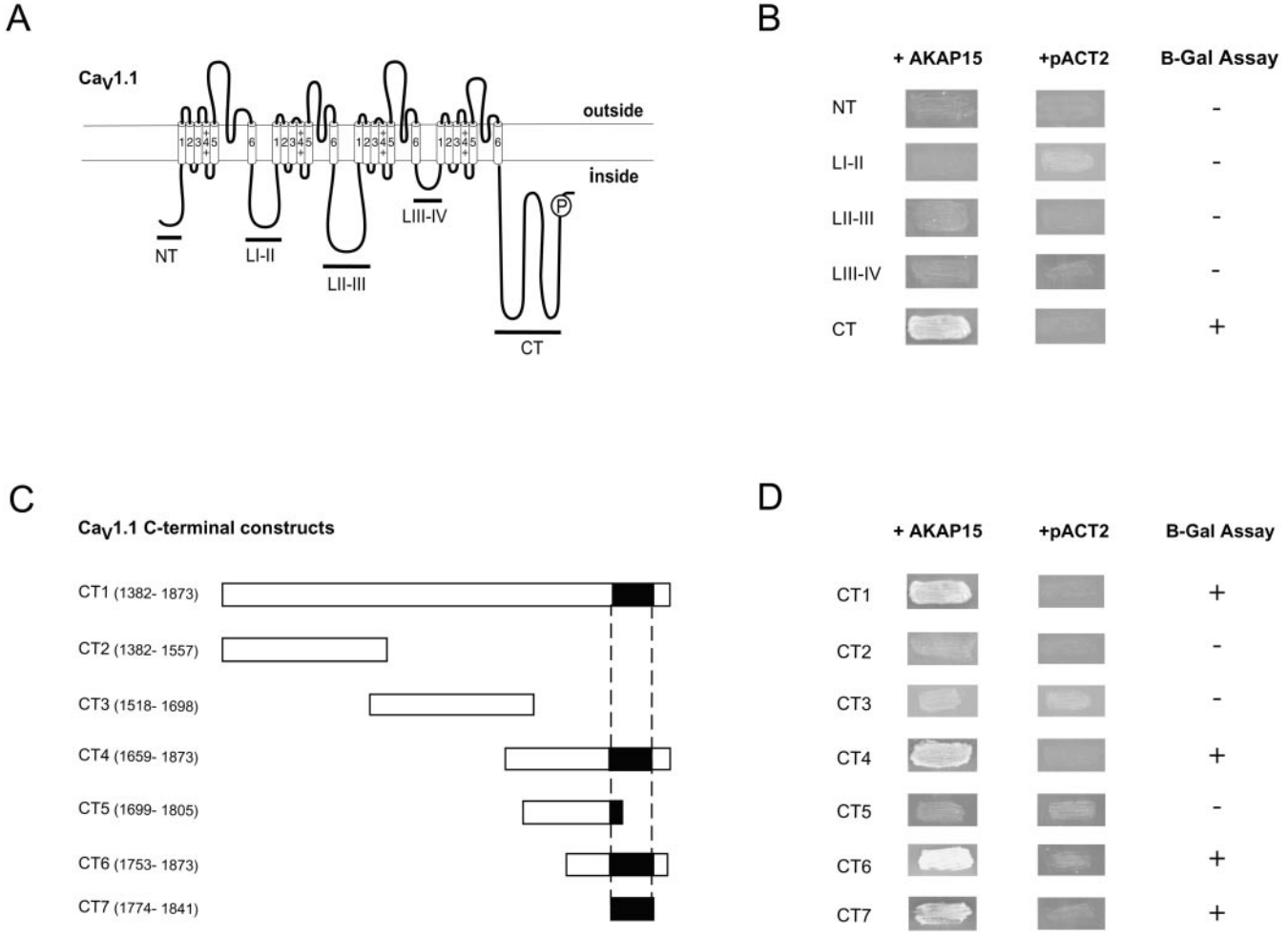

FIG. 1. **AKAP15 directly binds to the C-terminal domain of the α_1 subunit of skeletal muscle L-type Ca^{2+} channels ($Ca_V1.1$).** *A*, schematic diagram of the major intracellular domains of the α_1 subunit of $Ca_V1.1$ that were cloned into the pAS2.1 vector and co-transformed with AKAP15.pACT2 or pACT2 alone into the Y190 yeast strain. *B*, representative growth of yeast co-transformed with the $Ca_V1.1$ plasmids depicted in *A* and AKAP15.pACT2 or pACT2 plated on selective media ($trp^-leu^-his^-$ +30 mM 3-AT) following 7 days of incubation at 30 °C and the resulting β-galactosidase (*β-Gal*) activity of yeast co-transformed with the intracellular domains of $Ca_V1.1$ and AKAP15.pACT2 (+ or −). *C*, schematic map of the C-terminal (*CT*) constructs of $Ca_V1.1$ co-transformed with AKAP15.pACT2 or pACT2 alone. *Numbers* in *parentheses* correspond to the amino acid residues in the α_1 subunit of $Ca_V1.1$. *D*, representative growth of yeast co-transformed with the $Ca_V1.1$ plasmids depicted in *C* and resulting β-galactosidase activity (+ or −) as described in *B*.

C-terminal domain of $Ca_V1.1$ at a site located between residues 1753 and 1873, the boundaries of CT6. We did not examine CT7 in these experiments because of poor expression in bacteria.

To verify the interaction between AKAP15 and the C terminus of $Ca_V1.1$ *in vivo*, immunoprecipitation experiments were performed in mammalian cells. The N terminus of AKAP15 contains a consensus sequence for myristoylation and palmitoylation that is required for its insertion into the plasma membrane (12, 13). This N-terminal acylation (NAc) sequence of AKAP15 was engineered onto the N terminus of fusion proteins encompassing different regions of the C-terminal domain of $Ca_V1.1$ to target them to the plasma membrane (Fig. 3*A*), and their ability to interact with AKAP15 was examined by immunoprecipitation studies. TsA-201 cells were co-transfected with Myc-tagged NAc-CT constructs and AKAP15. Cell lysates were immunoprecipitated with an anti-Myc antibody or non-immune IgG, and the immunoprecipitated AKAP15 protein was detected with the anti-AP1 antibody. Immunoblotting of cell lysates with anti-AP1 or anti-Myc antibody demonstrated robust expression of AKAP15 and the NAc-CT constructs, respectively (Fig. 3*B*, *lower panels*). AKAP15 specifically co-immunoprecipitated with CT1, CT4, CT6, and CT7 but not CT3 (Fig. 3*B*, *upper panel*), consistent with our yeast two-hybrid data (Fig. 1). Furthermore, failure of AKAP15 to co-immunoprecipitate with CT3 rules out the possibility of nonspecific interactions due to the presence of the NAc sequence. Interestingly, AKAP15 also co-immunoprecipitated with CT8 (residues 1774–1821), suggesting that a 48-residue AKAP15 binding domain (ABD) in the distal C terminus of $Ca_V1.1$ is sufficient to interact with AKAP15. Taken together with the yeast two-hybrid and *in vitro* binding data, we can conclude that the ABD is located within residues 1774–1841, the boundaries of CT7, and probably is within residues 1774–1821, the boundaries of CT8.

Identification of Leucine Zipper-like (LZ) Motifs in AKAP15 and the $Ca_V1.1$ ABD—To identify the region within AKAP15 that binds to the $Ca_V1.1$ ABD, a series of constructs spanning different regions of AKAP15 were generated (Fig. 4), and their ability to interact with the $Ca_V1.1$ ABD was assessed using the yeast two-hybrid assay. A 27-amino acid fragment (residues 28–54) was sufficient to interact with the $Ca_V1.1$ ABD (Fig. 4). This region contains the amphipathic helix (residues 28–40) of AKAP15 that binds the type II regulatory subunit of PKA (12). However, the amphipathic region of AKAP15 was not sufficient to mediate the interaction, as deletion of the last 41 amino acids of AKAP15 (AKAP15(1–

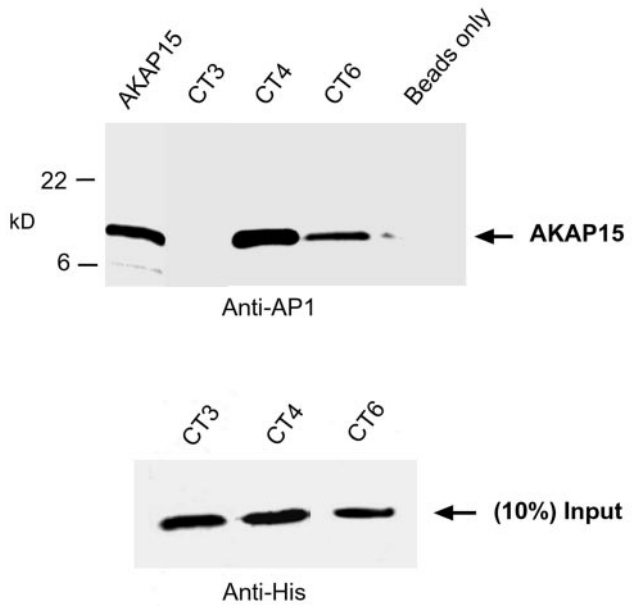

FIG. 2. ***In vitro* interaction of AKAP15 with the C-terminal domain of $Ca_V1.1$.** His fusion proteins, CT3, CT4, and CT6 of $Ca_V1.1$ (shown schematically in Fig. 1*C*), were immobilized on nickel-nitrilotriacetic acid-agarose and incubated with purified AKAP15. Following extensive washing, bound proteins were separated by SDS-PAGE and transferred to nitrocellulose. Bound AKAP15 was visualized by Western blot analysis with anti-AP1 antibody (*upper panel*). A fraction (10%) of the total amount of each CT fusion protein used in the binding assay was probed with the monoclonal anti-His antibody (*lower panel*) to show equivalent amounts of each protein used in the assay.

40)) abolished binding to the $Ca_V1.1$ ABD (Fig. 4). These results suggest that a region distal to the amphipathic region of AKAP15 interacts with the $Ca_V1.1$ ABD.

Secondary structure prediction analysis revealed that the helix of AKAP15 extends beyond the amphipathic region to form a coiled-coil, characterized by a leucine heptad motif (Fig. 5*A*). Leucine and isoleucine zipper (LZ) motifs are α-helical heptad repeats that have recently been implicated in mediating protein-protein interactions that target kinases and phosphatases to macromolecular complexes (20, 21). The region of AKAP15 (residues 28–54) identified as critical for binding to the $Ca_V1.1$ ABD contains a leucine heptad motif between residues 42 and 49, raising the possibility that AKAP15 interacts with the $Ca_V1.1$ ABD via its LZ motif.

If AKAP15 interacts with the $Ca_V1.1$ ABD via its LZ motif, then a similar LZ motif would be expected in the ABD of $Ca_V1.1$. Secondary structure prediction analysis revealed that this region of the Ca^{2+} channel has a high probability of forming an α-helix, interrupted by two glycine residues at positions 1795 and 1796 (Fig. 5*A*). Whereas the $Ca_V1.1$ ABD does not contain the "classical" LZ motif, it does contain a valine-leucine heptad motif between residues 1786 and 1814 (Fig. 5*A*), and valine residues have been identified in hydrophobic heptad zipper motifs in proteins (22–24).

AKAP15 Binds the C Terminus of $Ca_V1.1$ via a Novel LZ Interaction—Site-directed mutagenesis studies have shown that alanine substitutions of one or more leucine residues in LZ motifs greatly diminish the ability of LZ motifs to mediate protein-protein interactions without disrupting the overall α-helical structure (25, 26). To test the hypothesis that AKAP15 binds to the C-terminal domain of $Ca_V1.1$ via an LZ-like interaction, leucine residues in AKAP15 at positions 42 and 49 were mutated to alanine to generate $AKAP15_{LZM}$. In addition, valine and leucine residues at positions 1793 and 1800, respectively, were mutated to alanine to generate $Ca_V1.1$ ABD_{LZM}. These residues in the $Ca_V1.1$ ABD were chosen for mutagenesis because of their central location in the motif and because the "d" positions of heptad repeats are often important for mediating protein-protein interactions (27).

The ability of these mutants to interact was first examined using the yeast two-hybrid assay. Fig. 5*B* shows that alanine substitution of the leucine residues in the coiled-coil region of AKAP15 abolished the interaction with the $Ca_V1.1$ ABD (Fig. 5*B*, *upper panel*). Similarly, the $Ca_V1.1$ ABD_{LZM} mutant failed to interact with either *wt*AKAP15 or $AKAP15_{LZM}$ (Fig. 5*B*). Confirmation of these results were obtained in co-immunoprecipitation experiments. Lysates of tsA-201 cells co-expressing *wt*AKAP15 or $AKAP15_{LZM}$ with either the $Ca_V1.1$ ABD or $Ca_V1.1$ ABD_{LZM} were immunoprecipitated with an anti-Myc antibody or non-immune IgG, and the immunoprecipitated proteins were detected using the RII-biotin assay. We found that binding of either $AKAP15_{LZM}$ to *wt*$Ca_V1.1$ ABD or *wt*AKAP15 to $Ca_V1.1$ ABD_{LZM} was significantly diminished (Fig. 5*C*, *upper panel, lanes 2* and *3*). Furthermore, co-expression of $AKAP15_{LZM}$ with $Ca_V1.1$ ABD_{LZM} completely eliminated binding (Fig. 5*C*, *upper panel*, *lane 4*). Immunoblotting of cell lysates with RII-biotin or an anti-Myc antibody demonstrated robust expression of AKAP15 and the NAc-CT constructs, respectively (Fig. 5*C*, *lower panels*). Failure of $AKAP15_{LZM}$ to co-immunoprecipitate the $Ca_V1.1$ ABD_{LZM} was not due to disruption in the α-helical structure of the protein because RII retained its ability to bind the amphipathic helix of $AKAP15_{LZM}$ (Fig. 5*C*, *lower left panel*). A synthetic peptide corresponding to the LZ motif of AKAP15 (residues 38–54; $AKAP15_{LZ}$(38–54)) was generated and used in peptide competition co-immunoprecipitation experiments. Lysates of tsA-201 cells co-expressing *wt*AKAP15 and the $Ca_V1.1$ ABD were first incubated either in the presence or absence of the $AKAP15_{LZ}$(38–54) peptide, immunoprecipitated with an anti-Myc antibody or non-immune IgG, and the immunoprecipitated AKAP15 protein was detected with the anti-AP1 antibody. As shown in Fig. 5*D*, pre-incubation of cell lysates with the $AKAP15_{LZ}$(38–54) peptide abolished co-immunoprecipitation of AKAP15 with the $Ca_V1.1$ ABD. Taken together, these data provide strong evidence that AKAP15 and the $Ca_V1.1$ ABD specifically interact via their LZ-like motifs.

AKAP15 Binding to L-type Ca^{2+} Channels via LZ Interactions Enhances Voltage-dependent Potentiation in Skeletal Myotubes—Previous studies (4, 14, 15) have shown that voltage-dependent potentiation of L-type Ca^{2+} channel activity in skeletal muscle cells requires anchoring of PKA near Ca^{2+} channels. To examine the functional role of the LZ interaction between AKAP15 and the C-terminal domain of $Ca_V1.1$, we chose the well-differentiated mouse MM14 skeletal muscle cell line (28).

To confirm that voltage-dependent potentiation of L-type Ca^{2+} channels was present in MM14 myotubes, we used the following pulse protocol. Potentiation induced by a 200-ms conditioning prepulse to +100 mV was measured by comparing the amplitude of barium currents (I_{Ba}) elicited by test pulses to variable voltages before and after the conditioning prepulse (Fig. 6*A*). In the absence of a conditioning prepulse, little I_{Ba} was elicited during a test pulse to −10 mV (Fig. 6*A*, *P1*). In contrast, I_{Ba} elicited in response to an identical test pulse was strongly potentiated when preceded by a depolarizing prepulse to +100 mV (Fig. 6*A*, *P2*). Currents were normalized to the largest current elicited during the first test pulses (P1) and the normalized currents were plotted as a function of test voltage. Fig. 6*A* (*lower panel*) shows that potentiation was strongly voltage-dependent; potentiation was most evident during test

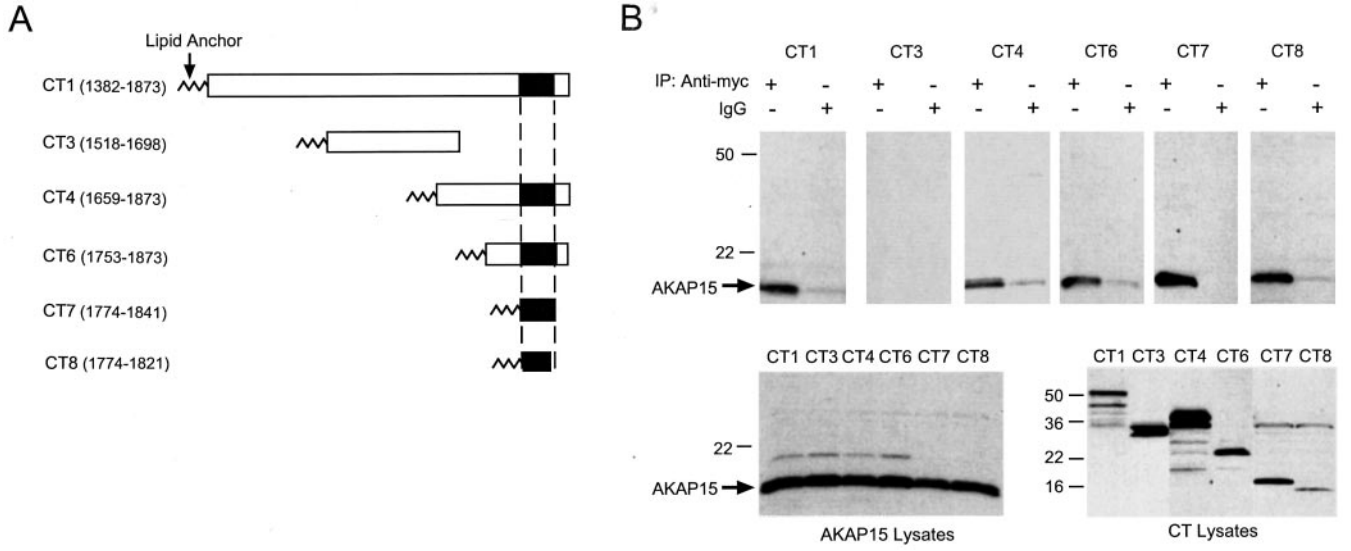

FIG. 3. **Co-immunoprecipitation of AKAP15 with the C-terminal domain of $Ca_V1.1$ in tsA-201 cells.** *A*, schematic diagram of the lipid-anchored CT constructs of $Ca_V1.1$ examined in co-immunoprecipitation studies. *Numbers* in *parentheses* correspond to the amino acid residues in the α_1 subunit of $Ca_V1.1$. *B*, TsA-201 cells were co-transfected with the Myc-tagged CT constructs depicted in *A* plus AKAP15, and cell lysates were immunoprecipitated (*IP*) with the monoclonal anti-Myc antibody or control IgG. Following SDS-PAGE and transfer to nitrocellulose, blots were probed with anti-AP1 antibody (*upper panel*) to detect AKAP15. *Lower panel*, lysates from transfected cells were probed with either monoclonal anti-Myc antibody (*right*) or anti-AP1 antibody (*left*) to verify expression of each protein.

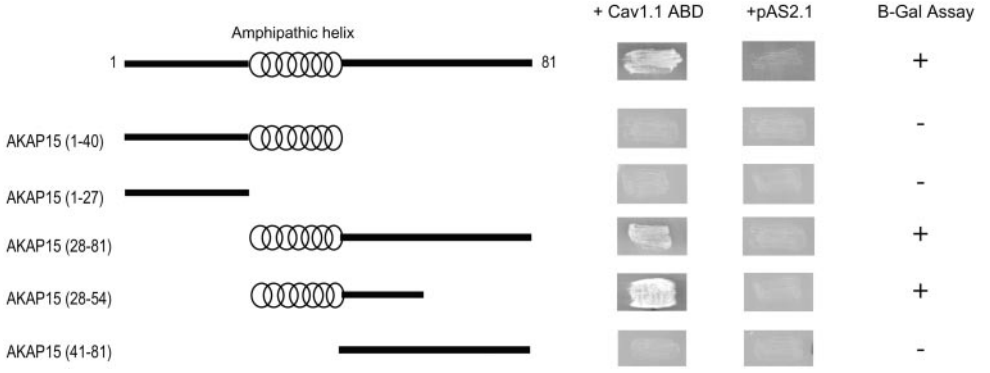

FIG. 4. **Amino acid residues 28–54 of AKAP15 are sufficient to bind the $Ca_V1.1$ ABD.** *Left panel*, schematic map of the AKAP15.pACT2 constructs co-transformed with the $Ca_V1.1$ ABD.pAS2.1 into the Y190 yeast strain. *Numbers* in *parentheses* correspond to the amino acid residues in AKAP15. *Right panel*, representative growth of yeast co-transformed with the AKAP15 plasmids and the $Ca_V1.1$ ABD and plated on selective media ($trp^-leu^-his^-$ + 30 mM 3-AT) following 7 days of incubation at 30 °C and the resulting β-galactosidase (*β-Gal*) activity (+ or −) of yeast co-transformed with AKAP15.pACT2 and $Ca_V1.1$ ABD.pAS2.1.

pulses between −20 and 0 mV with no detectable potentiation at potentials more positive than +20 mV. Furthermore, prepulse potentiation caused a −14.2 ± 1.5 mV hyperpolarizing shift in the I-V curve and an increase in the steepness of the activation curve. These characteristics are in agreement with previous reports of prepulse potentiation of skeletal muscle L-type Ca^{2+} channels in other cell systems (4, 14, 15).

To confirm that anchoring of PKA near Ca^{2+} channels is required for the prepulse potentiation observed in MM14 cells, we examined the effects of PKI(5–24), a specific peptide inhibitor of PKA, and AP2, a peptide inhibitor of the PKA-AKAP15 interaction on prepulse potentiation. As reported previously (4, 12, 14), dialysis of either 10 μM PKI (Fig. 6*B*) or 100 μM AP2 into skeletal MM14 cells (Fig. 6*C*) substantially reduced prepulse potentiation at all voltages tested. Mean potentiation measured at −10 mV was 7.28 ± 0.137-fold in the absence of peptide compared with 3.39 ± 0.321- and 2.1 ± 0.077-fold in the presence of PKI and AP2, respectively (Fig. 6*F*). Both PKI and AP2 blocked the hyperpolarizing shift in the voltage dependence of activation. Furthermore, in the absence of a conditioning prepulse, dialysis of either PKI or AP2 produced a small shift in the voltage dependence of activation toward more positive potentials (Fig. 6, *B* and *C*). These results are consistent with the hypothesis that PKA anchoring close to Ca^{2+} channels is required for voltage-dependent potentiation of skeletal muscle L-type Ca^{2+} channels (12, 14, 15).

Having established the importance of PKA anchoring in voltage-dependent potentiation in MM14 skeletal myotubes, the functional significance of AKAP15 binding to the C-terminal domain of $Ca_V1.1$ was examined. The synthetic peptide corresponding to the LZ motif of AKAP15 ($AKAP15_{LZ}$(38–54)), which binds to the $Ca_V.1.1$ ABD *in vitro* (Fig. 5*D*), was introduced into the intracellular pipette solution. In cells dialyzed with 100 μM $AKAP15_{LZ}$(38–54), prepulse potentiation was greatly reduced, and the hyperpolarizing shift in the voltage dependence of activation was significantly blocked (Fig. 6*D*). Moreover, $AKAP15_{LZ}$(38–54) reduced potentiation as effectively as PKI since potentiation measured at −10 mV was 3.22 ± 0.173 (Fig. 6*F*). In contrast, dialysis of a mutant form of the same peptide, in which alanine residues were substituted for the two critical leucine residues ($AKAP15_{LZm}$(38–54)), had no significant effect on potentiation (Fig. 6, *E* and *F*). Thus, our data show that targeting of PKA to Ca^{2+} channels via a novel LZ-like interaction between AKAP15 and the C-terminal do-

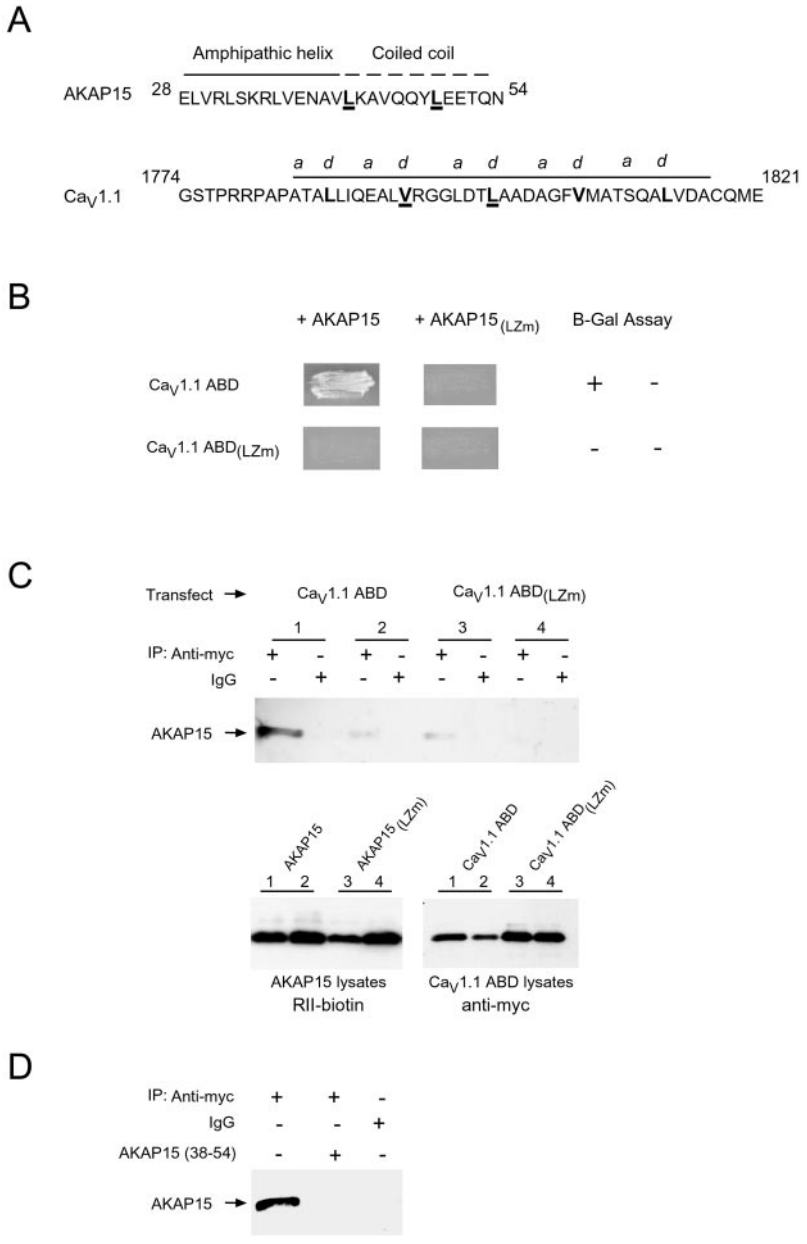

FIG. 5. **AKAP15 binds to the $Ca_V1.1$ ABD via LZ-like motifs.** *A*, amino acid sequences of the binding domains of AKAP15 and the $Ca_V1.1$ ABD. LZ motifs identified in AKAP15 and the $Ca_V1.1$ ABD are highlighted in *bold*, and the amino acid residues that were mutated are *underlined*. Leucine residues in AKAP15 at positions 42 and 49 were mutated to alanine to generate $AKAP15_{LZM}$, and valine and leucine residues at positions 1793 and 1800 in $Ca_V1.1$ ABD were mutated to alanine to generate $Ca_V1.1ABD_{LZM}$. *B*, the ability of *wt*$Ca_V1.1$ ABD and $Ca_V1.1$ ABD_{LZM} to interact with *wt*AKAP15 and $AKAP15_{LZM}$ was examined using the yeast two-hybrid assay. Representative yeast growth on selective media ($trp^-leu^-his^-$ + 30 mM 3-AT) following 7 days of incubation at 30 °C and the resulting β-galactosidase (*β-Gal*) activity (+ or −) are shown. *C*, TsA-201 cells were co-transfected with *wt*$Ca_V1.1$ ABD and *wt*AKAP15 (*lane 1*), *wt*$Ca_V1.1$ ABD and $AKAP15_{LZM}$ (*lane 2*), $Ca_V1.1$ ABD_{LZM} and *wt*AKAP15 (*lane 3*), or $Ca_V1.1$ $AB-D_{LZM}$ and $AKAP15_{LZM}$ (*lane 4*). Cell lysates were immunoprecipitated (*IP*) with an anti-Myc antibody or non-immune IgG, and the immunoprecipitated AKAP15 protein was detected using the RII-biotin assay (*upper panel*). Immunoblotting of cell lysates with RII-biotin (*lower left panel*) or an anti-Myc antibody (*lower right panel*) shows equivalent expression of the AKAP15 and $Ca_V1.1$ ABD protein, respectively. *D*, lysates of tsA-201 cells co-expressing *wt*AKAP15 and the $Ca_V1.1$ ABD were incubated either in the presence or absence of 1 mM $AKAP15_{LZ}$(38–54) peptide for 1 h at 4 °C and then immunoprecipitated with an anti-Myc antibody or non-immune IgG. Immunoprecipitated AKAP15 protein was detected with the anti-AP1 antibody.

main of $Ca_V1.1$ plays an important role in voltage-dependent potentiation of skeletal muscle L-type Ca^{2+} channels.

DISCUSSION

Our results make three advances toward understanding the molecular mechanism of regulation of skeletal muscle Ca^{2+} channels by cAMP-dependent protein phosphorylation. First, we show that AKAP15 targets PKA to the C-terminal domain of $Ca_v1.1$ by a direct protein-protein interaction. Second, we show that this interaction is mediated by a novel site through modified leucine zipper motifs in AKAP15 and in the C-terminal domain of the $Ca_V1.1$ channel. Third, we find that mutation of this motif prevents kinase anchoring, and disruption of this interaction in skeletal muscle cells with dominant-negative peptides prevents PKA- and voltage-dependent potentiation of Ca^{2+} channel activity. Our results provide the first evidence for voltage-gated ion channel regulation by direct targeting of PKA and AKAP to a specific site of phosphorylation and reveal a novel paradigm for rapid and precise modulation of ion channel activity. These points are considered in more detail below.

Direct Association of AKAP15 with the C-terminal Domain of the α_1 Subunit of $Ca_V1.1$—Although previous work (12, 16) has shown that AKAP15 co-purifies, co-immunoprecipitates, and co-localizes with the α_1 subunit of $Ca_V1.1$, the mechanism by which AKAP15 associates with the Ca^{2+} channel complex has not been elucidated. Our studies reveal that AKAP15 directly interacts with the C-terminal domain of the α_1 subunit of $Ca_V1.1$. Deletion analysis identified a 48-amino acid region (residues 1774–1821) in the distal half of the C-terminal domain of $Ca_V1.1$ that is sufficient for the interaction with AKAP15 (Fig. 3). Two size forms of the α_1 subunit of $Ca_V1.1$, ~190 and 212 kDa, exist in native skeletal muscle preparations, and both are phosphorylated by PKA in intact cells (29–32). The predominant short form results from posttranslational cleavage in the C-terminal domain between residues 1685 and 1699 (30). The finding that the AKAP15 interaction site in $Ca_V1.1$ is located in the C-terminal domain that is cleaved in the truncated form of $Ca_V1.1$ is surprising, particularly since our functional data show that disruption of the

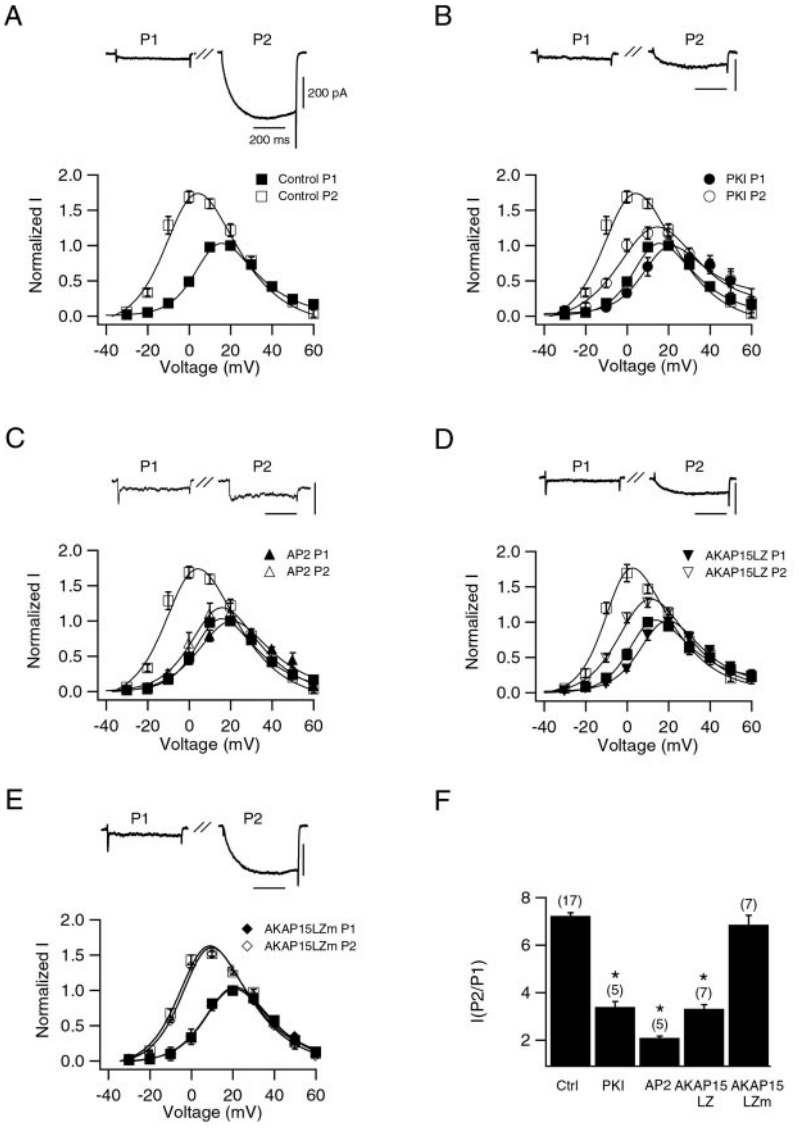

FIG. 6. **Effect of PKI, AP2, and $AKAP15_{LZ}$ on prepulse potentiation of L-type Ca^{2+} channels in MM14 skeletal myotubes.** Currents were elicited by a 300-ms test pulse (*P1*) to a potential between −40 and +60 mV (potential varied in 10 mV steps). After a 3-s interval at a holding potential of −80 mV, a 200-ms conditioning prepulse to +100 mV was applied, which was immediately followed by a brief 25-ms repolarization to −60 mV and then a second test pulse (*P2*) to the same potential as P1. *A–E*, *upper panel*, representative currents elicited by 300-ms test pulses to −10 mV before (*P1*) and after (*P2*) the conditioning prepulse to +100 mV. *Lower panel*, normalized current-voltage relationships (mean ± S.E.) of I_{Ba} before (*closed symbols*) and after (*open symbols*) the conditioning prepulse. Current measured at the end of each test pulse was normalized to the largest current elicited during the first test pulses (P1), and the normalized currents were plotted as a function of voltage. *A*, prepulse potentiation of I_{Ba} in the absence of peptide dialysis ($n = 17$). The effects of PKI (10 μM; $n = 5$, *B*), AP2 (100 μM; $n = 5$, *C*), $AKAP15_{LZ}$(38–54) (100 μM; $n = 7$, *D*), and $AKAP15_{LZm}$(38–54) (100 μM; $n = 7$, *E*) on prepulse potentiation are compared to control (*squares*). The small inward current detected at the beginning of each representative current trace is T-type Ca^{2+} current present in these cells. *F*, the mean ratio of current (P2/P1) measured at the end of the test pulse at −10 mV is plotted for each condition (± S.E.)

interaction between AKAP15 and the C-terminal ABD of $Ca_V1.1$ greatly reduces voltage-dependent potentiation of the L-type Ca^{2+} channels in skeletal myotubes (Fig. 6*D*). These results imply that the distal C-terminal domain containing the $Ca_V1.1$ ABD remains associated with the body of the channel. These findings are consistent with recent reports on cardiac L-type Ca^{2+} channels ($Ca_V1.2$) suggesting that the cleaved distal C-terminal domain remains associated with the truncated α_1 subunit following proteolytic processing and regulates channel activity (33, 34).

A Novel LZ-like Interaction Mediates AKAP15 Binding to Skeletal Muscle L-type Ca^{2+} Channels—Deletion analysis of AKAP15 identified a 27-amino acid fragment (residues 28–54) that interacts with the C-terminal domain of $Ca_V1.1$ (Fig. 4). This region contains the amphipathic helix (residues 28–40) of AKAP15 that binds the type II regulatory subunit of PKA (12, 13). Truncation of the last 41 amino acids of AKAP15 abolished binding to the $Ca_V1.1$ ABD (Fig. 4) suggesting that a region distal to the amphipathic helix of AKAP15 interacts with the $Ca_V1.1$ ABD. Secondary structure analysis of AKAP15 revealed that the helical region of AKAP15 extends beyond the amphipathic helix (amino acids 28–40) to form a coiled-coil, characterized by a leucine heptad motif (Fig. 5*A*). Leucine and isoleucine zipper motifs are α-helical heptad repeats that were originally identified in transcription factors and shown to mediate their homo- and heterodimerization (35, 36). Moreover, a role for LZ motifs in mediating protein-protein interactions that target kinases and phosphatases to macromolecular complexes has recently emerged (20, 21), raising the possibility that AKAP15 interacts with the C-terminal domain of $Ca_V1.1$ via an LZ-like interaction. Secondary structure prediction analysis of the $Ca_V1.1$ ABD revealed that this region has a high probability of forming an α-helix, interrupted by two glycine residues positioned at 1795 and 1796 (Fig. 5*A*). Although the $Ca_V1.1$ ABD does not contain the "classical" LZ motif, it does contain a valine-leucine zipper motif between residues 1786 and 1814 (Fig. 5*A*). In the present study, site-directed mutagenesis revealed that alanine substitution of either the leucine residues in AKAP15 or valine/leucine residues in the $Ca_V1.1$ ABD abolished the interaction between the two proteins (Fig. 5, *B* and *C*), supporting a novel role of LZ-like motifs in associating AKAP15 to skeletal muscle L-type Ca^{2+} channels.

Sequence alignment of the LZ-like region of $Ca_V1.1$ with other members of the Ca_V1 family revealed a striking conservation of LZ-like motifs among this family of Ca^{2+} channels,

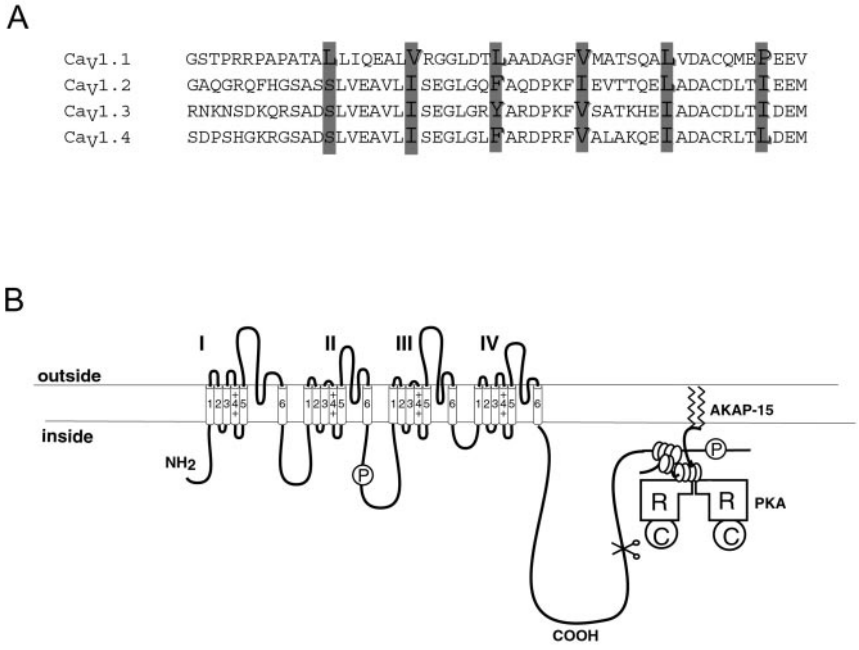

FIG. 7. **Conserved LZ motifs in the Ca_V1 family of voltage-gated Ca^{2+} channels.** *A*, amino acid sequence alignment of the LZ-like region identified in the C-terminal domain of $Ca_V1.1$ with other members of the Ca_V1 family. Conserved leucine residues or hydrophobic residues in the "a" and "d" positions of the heptad repeats are *shaded. B*, model of the LZ interaction between AKAP15 and the C-terminal domain of $Ca_V1.1$. AKAP15 directly associates with the C-terminal domain of $Ca_V1.1$ via an LZ-like interaction, where it strategically positions PKA close to a major PKA phosphorylation site located in $Ca_V1.1$ at serine 1854. Direct anchoring of PKA to Ca^{2+} channels via LZ interactions may provide a novel mechanism that ensures rapid and efficient phosphorylation of Ca^{2+} channels in response to local signals such as cAMP and depolarization.

with the exception of $Ca_V1.3$ where a tyrosine residue replaces a more hydrophobic residue in the heptad repeat (Fig. 7*A*). These data suggest that the association of AKAP15 (and possibly other AKAPs) with the C-terminal domains of Ca_V1 channels via LZ-like motifs may define a general mechanism for the precise targeting of PKA for regulation of L-type Ca^{2+} channels.

Our studies complement a recent report (21) identifying a novel role of LZ motifs in targeting kinases and phosphatases to the ryanodine-sensitive Ca^{2+}-release channel of the sarcoplasmic reticulum by adding the family of voltage-gated Ca^{2+} channels to the growing list of targets for this mode of localization of signaling complexes. Together, these studies suggest that targeting of kinases (and phosphatases) to ion channels via LZ-like motifs defines a general mechanism that allows greater speed and precision in ion channel regulation.

Disruption of the LZ-like Interaction between AKAP15 and L-type Ca^{2+} Channels Reduces Voltage-dependent Potentiation in Skeletal Muscle Cells—Previous work (12, 14, 15) has shown that voltage-dependent potentiation of skeletal muscle L-type Ca^{2+} channels requires PKA that is anchored near the channel by AKAP15. In support of this hypothesis, we demonstrate that PKI and AP2, inhibitor peptides of PKA and the PKA-AKAP15 interaction, respectively, effectively reduce voltage-dependent potentiation of Ca^{2+} channels in skeletal muscle myotubes (Fig. 6, *B* and *C*). Furthermore, we show that disruption of the LZ interaction between AKAP15 and the C-terminal ABD of $Ca_V1.1$ is equally effective in reducing voltage-dependent potentiation (Fig. 6*D*). Taken together, these data suggest that anchoring of PKA to Ca^{2+} channels via LZ-like interactions plays a critical role in regulating skeletal muscle L-type Ca^{2+} channels. Identification of a novel role of LZ-like motifs in anchoring PKA to L-type Ca^{2+} channels sheds new light on the specificity and complexity of PKA regulation of ion channels.

Our results support a model that is illustrated in Fig. 7*B*. AKAP15 directly associates with the C-terminal domain of $Ca_V1.1$ via a LZ-like interaction, where it strategically positions PKA close to a major PKA phosphorylation site located in $Ca_V1.1$ at serine 1854. Thus, direct anchoring of PKA to L-type Ca^{2+} channels via LZ interactions provides a novel mechanism that ensures rapid and efficient phosphorylation of Ca^{2+} channels in response to local signals such as cAMP and depolarization. This increase in Ca^{2+} channel activity may play a critical role in regulating contractile force in response to hormones and to the frequency of stimulation by the motor nerve.

Acknowledgments—We thank John Angello for excellent skeletal myotube culture assistance and Teddy Lin for technical assistance.

REFERENCES

1. Catterall, W. A. (1991) *Cell* **64,** 871–874
2. Adams, B. A., and Beam, K. G. (1990) *FASEB J.* **4,** 2809–2816
3. Rios, E., and Pizarro, G. (1991) *Physiol. Rev.* **71,** 849–908
4. Sculptoreanu, A., Scheuer, T., and Catterall, W. A. (1993) *Nature* **364,** 240–243
5. Fleig, A., and Penner, R. (1995) *J. Physiol. (Lond.)* **489,** 41–53
6. Kernell, D., Eerbeek, O., and Verhey, B. A. (1983) *Exp. Brain Res.* **50,** 220–227
7. Arreola, J., Calvo, J., Garcia, M. C., and Sánchez, J. A. (1987) *J. Physiol. (Lond.)* **393,** 307–330
8. Carr, D. W., Hausken, Z. E., Fraser, I. C. D., Stofko-Hahn, R. E., and Scott, J. D. (1992) *J. Biol. Chem.* **267,** 13376–13382
9. Hausken, Z. E., Coghlan, V. M., Hastings, C. A., Reimann, E. M., and Scott, J. D. (1994) *J. Biol. Chem.* **269,** 24245–24251
10. Hausken, Z. E., and Scott, J. D. (1996) *Biochem. Soc. Trans.* **24,** 986–991
11. Newlon, M. G., Roy, M., Hausken, Z. E., Scott, J. D., and Jennings, P. A. (1997) *J. Biol. Chem.* **272,** 23637–23644
12. Gray, P. C., Johnson, B. D., Westenbroek, R. E., Hays, L. G., Yates, I. J., Scheuer, T., Catterall, W. A., and Murphy, B. J. (1998) *Neuron* **20,** 1017–1026
13. Fraser, I. D. C., Tavalin, S. J., Lester, L. B., Langeberg, L. K., Westphal, A. M., Dean, R. A., Marrion, N. V., and Scott, J. D. (1998) *EMBO J.* **17,** 2261–2272
14. Johnson, B. D., Scheuer, T., and Catterall, W. A. (1994) *Proc. Natl. Acad. Sci. U. S. A.* **91,** 11492–11496
15. Johnson, B. D., Brousal, J. P., Peterson, B. Z., Gallombardo, P. A., Hockerman, G. H., Lai, Y., Scheuer, T., and Catterall, W. A. (1997) *J. Neurosci.* **17,** 1243–1255
16. Gray, P. C., Tibbs, V. C., Catterall, W. A., and Murphy, B. J. (1997) *J. Biol. Chem.* **272,** 6297–6302
17. Burton, K. A., Johnson, B. D., Hausken, Z. E., Westenbroek, R. E., Idzerda, R. L., Scheuer, T., Scott, J. D., Catterall, W. A., and McKnight, G. S. (1997) *Proc. Natl. Acad. Sci. U. S. A.* **94,** 11067–11072
18. Bartel, P. L., Chien, C.-T., Sternglanz, R., and Fields, S. (1993) *Cellular Interactions in Development: A Practical Approach* (Hartley, D., ed) pp. 153–179, Oxford University Press, Oxford
19. Neville, C., Rosenthal, N., McGrew, M., Bogdanova, N., and Hauschka, S. (1998) *Methods Cell Biol.* **52,** 85–116
20. Surks, H. K., Mochizuki, N., Kasai, Y., Georgescu, S. P., Tang, K. M., Ito, M., Lincoln, T. M., and Mendelsohn, M. E. (1999) *Science* **286,** 1583–1587
21. Marx, S. O., Reiken, S., Hisamatsu, Y., Gaburjakova, M., Gaburjakova, J., Yang, Y. M., Rosemblit, N., and Marks, A. R. (2001) *J. Cell Biol.* **153,** 699–708
22. Yu, M., Miller, R. H., Emerson, S., and Purcell, R. H. (1996) *J. Virol.* **70,** 7085–7091
23. Stone-Hulslander, J., and Morrison, T. G. (1999) *J. Virol.* **73,** 3630–3637
24. Stefancsik, R., Jha, P. K., and Sarkar, S. (1998) *Proc. Natl. Acad. Sci. U. S. A.* **95,** 957–962
25. Simmerman, H. K., Kobayashi, Y. M., Autry, J. M., and Jones, L. R. (1996)

J. Biol. Chem. **271,** 5941–5946
26. Moitra, J., Szilak, L., Krylov, D., and Vinson, C. (1997) *Biochemistry* **36,** 12567–12573
27. Hurst, H. C. (1995) *Protein Profile* **2,** 101–168
28. Hauschka, S. D., Linkhart, T. A., Clegg, C., and Merrill, G. (1979) *Muscle Regeneration. Clonal Studies of Human and Mouse Muscle* (Mauro, A., ed) pp. 311–322, Raven Press, Ltd., New York
29. De Jongh, K. S., Merrick, D. K., and Catterall, W. A. (1989) *Proc. Natl. Acad. Sci. U. S. A.* **86,** 8585–8589
30. De Jongh, K. S., Warner, C., Colvin, A. A., and Catterall, W. A. (1991) *Proc. Natl. Acad. Sci. U. S. A.* **88,** 10778–10782
31. Lai, Y., Seagar, M. J., Takahashi, M., and Catterall, W. A. (1990) *J. Biol. Chem.* **265,** 20839–20848
32. Rotman, E. I., De Jongh, K. S., Florio, V., Lai, Y., and Catterall, W. A. (1992) *J. Biol. Chem.* **267,** 16100–16105
33. Gerhardstein, B. L., Gao, T., Bunemann, M., Puri, T. S., Adair, A., Ma, H., and Hosey, M. M. (2000) *J. Biol. Chem.* **275,** 8556–8563
34. Gao, T., Cuadra, A. E., Ma, H., Bunemann, M., Gerhardstein, B. L., Cheng, T., Eick, R. T., and Hosey, M. M. (2001) *J. Biol. Chem.* **276,** 21089–21097
35. Turner, R., and Tjian, R. (1989) *Science* **243,** 1689–1694
36. Landschulz, W. H., Johnson, P. F., and McKnight, S. L. (1988) *Science* **240,** 1759–1764